

Design, Synthesis, Biological Evaluation, and Structural Characterization of Potent Histone Deacetylase Inhibitors Based on Cyclic α/β -Tetrapeptide Architectures

Ana Montero, John M. Beierle, Christian A. Olsen, and M. Reza Ghadiri*

Department of Chemistry and The Skaggs Institute for Chemical Biology, The Scripps Research Institute, 10550 North Torrey Pines Road, La Jolla, California 92037

Received December 5, 2008; E-mail: ghadiri@scripps.edu

Abstract: Histone deacetylases (HDACs) are a family of enzymes found in bacteria, fungi, plants, and animals that profoundly affect cellular function by catalyzing the removal of acetyl groups from ϵ -*N*-acetylated lysine residues of various protein substrates including histones, transcription factors, α -tubulin, and nuclear importers. Although the precise roles of HDAC isoforms in cellular function are not yet completely understood, inhibition of HDAC activity has emerged as a promising approach for reversing the aberrant epigenetic states associated with cancer and other chronic diseases. Potent new isoform-selective HDAC inhibitors would therefore help expand our understanding of the HDAC enzymes and represent attractive lead compounds for drug design, especially if combined with high-resolution structural analyses of such inhibitors to shed light on the three-dimensional pharmacophoric features necessary for the future design of more potent and selective compounds. Here we present structural and functional analyses of a series of β -amino-acid-containing HDAC inhibitors inspired by cyclic tetrapeptide natural products. To survey a diverse ensemble of pharmacophoric configurations, we systematically varied the position of the β -amino acid, amino acid chirality, functionalization of the Zn^{2+} -coordinating amino acid side chain, and alkylation of the backbone amide nitrogen atoms around the macrocycle. In many cases, the compounds were a single conformation in solution and exhibited potent activities against a number of HDAC isoforms as well as effective antiproliferative and cytotoxic activities against human tumor cells. High-resolution NMR solution structures were determined for a selection of the inhibitors, providing a useful means of correlating detailed structural information with potency. The structure-based approach described here is expected to furnish valuable insights toward the future design of more selective HDAC inhibitors.

Introduction

Class-I, -II, and -IV histone deacetylases (HDACs) are Zn^{2+} -dependent enzymes that catalyze the removal of acetyl groups from ϵ -*N*-acetylated lysine residues of various protein substrates. These enzymes consequently play key roles in the epigenetic regulation of gene expression and modulating diverse cellular processes.^{1–6} Although the primary target of HDACs appear to be the ϵ -*N*-acetyl-lysine residues in histone tails, which affect the packing of chromatin complexes and thereby govern gene transcription, HDACs also regulate the functions of a growing list of nonhistone proteins.³ These include α -tubulin in microtubules, the oncosuppressor p53 and other transcription factors, and nuclear importer proteins. Indeed, it has even been postulated that the principle substrate for some HDAC enzymes are not the histone proteins themselves but rather one of these nonhistone protein substrates.³ The precise roles of the individual

HDAC isoforms in cellular function and tumorigenesis are not yet completely understood and are an area of intense research. New potent and selective HDAC inhibitors would serve as useful tools to help clarify these issues.

Owing to the diverse, fundamental cellular processes regulated by the HDACs, it is not surprising that inhibition of HDAC activity has emerged as a promising approach for reversing the anomalous epigenetic states associated with cancer and other chronic diseases.^{1–3,6} A number of HDAC inhibitors have entered clinical trials,¹ with SAHA (vorinostat)⁷ recently approved by the FDA for treatment of cutaneous T-cell lymphoma. Aside from medicinal applications, HDAC inhibitors were also pivotal in the purification and cloning of the mammalian HDAC enzymes.^{6,8} Therefore, the development of new HDAC inhibitors could deliver new methods to identify novel HDAC enzymes as well as uncover protein substrates and pathways regulated by HDAC enzymes. Most HDAC inhibitors are nonspecific across the family of enzymes, even though the ability to selectively inhibit individual HDAC isoforms would facilitate identification of the particular roles of each HDAC subtype in cellular processes and antitumor activities and undoubtedly also

(1) Paris, M.; Porcelloni, M.; Binaschi, M.; Fattori, D. *J. Med. Chem.* **2008**, *51*, 1505–1529.

(2) Bieliauskas, A. V.; Pflum, M. K. H. *Chem. Soc. Rev.* **2008**, *37*, 1402–1413.

(3) Minucci, S.; Pelicci, P. G. *Nat. Rev. Cancer* **2006**, *6*, 38–51.

(4) de Ruijter, A. J. M.; van Gennip, A. H.; Caron, H. N.; Kemp, S.; van Kuilenburg, A. B. P. *Biochem. J.* **2003**, *370*, 737–749.

(5) Verdin, E.; Dequiedt, F.; Kasler, H. G. *Trends Genet.* **2003**, *19*, 286–293.

(6) Meinke, P. T.; Liberator, P. *Curr. Med. Chem.* **2001**, *8*, 211–235.

(7) Marks, P. A.; Breslow, R. *Nat. Biotechnol.* **2007**, *25*, 84–90.

(8) Taunton, J.; Hassig, C. A.; Schreiber, S. L. *Science* **1996**, *272*, 408–11.

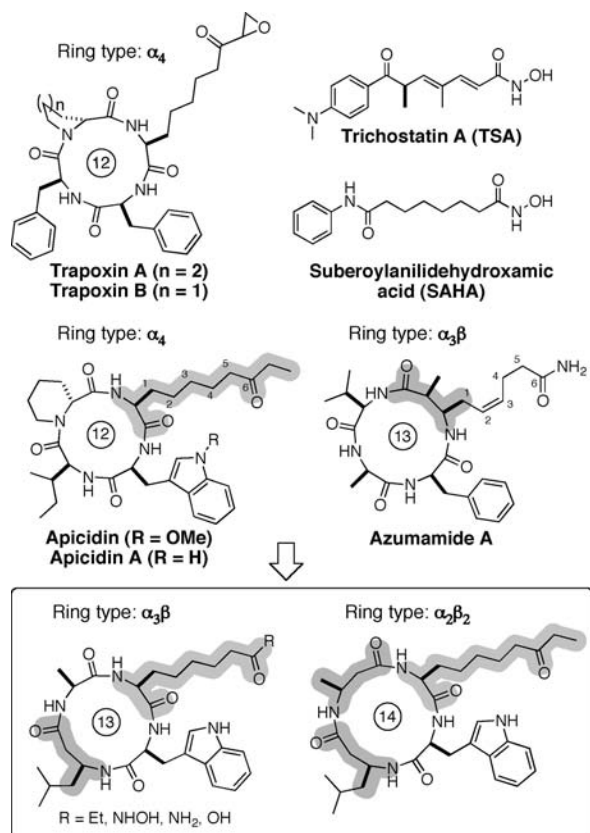


Figure 1. Chemical structures of selected natural and synthetic HDAC inhibitors. General structures of the β -amino-acid-containing cyclic peptides described here are also shown (boxed).

represent attractive drug candidates. Unfortunately, the design of selective HDAC inhibitors is currently hampered by a paucity of knowledge of the structural differences between HDAC isoforms and a limited number of cocrystal structures for the HDACs with inhibitor compounds. Thus far, cocrystal structures have been determined for only "HDAC-like protein" (HDLP),⁹ the catalytic domain of HDAC7,¹⁰ and HDAC8,¹¹ all of which were cocrystallized with trichostatin A (TSA).

An interesting family of HDAC inhibitors is the nonribosomal cyclic tetrapeptide natural products, including the apicidins, azumamides, trapoxins, HC-toxins, and chlamydocin (Figure 1).^{3,6,12} These inhibitors contributed significantly to the isolation and understanding of the HDAC enzymes; a trapoxin affinity matrix, for example, was used to isolate and purify the first mammalian HDAC enzyme.⁸ The cyclic tetrapeptide inhibitors are distinguished by the presence of a functionally critical Zn^{2+} -coordinating amino acid side chain containing a terminal α,β -epoxyketone, ethylketone, amide, or carboxylic acid. These

unnatural amino acids are approximately isosteric with an acetylated Lys and therefore almost certainly function by both mimicking an acetylated Lys residue of a substrate protein and interacting with the active site zinc ion. The epoxyketone functionalization was initially deemed a requirement for these inhibitors because it was present in all the earliest discovered members of the family, although more recently potent irreversible inhibitors lacking the epoxide, such as the apicidins and azumamides, have been discovered. The differing cytotoxic potencies of the various cyclic tetrapeptide inhibitors are thought to stem from a number of factors including the type of functionalization of the Zn^{2+} -coordinating amino acid residue,⁶ the predominant peptide backbone conformation in solution,^{12,13} and the overall peptide polarity resulting in differing capacities for the inhibitors to cross cellular and nuclear membranes.¹⁴ Aside from the Zn^{2+} -coordinating residue, the cyclic tetrapeptide inhibitors typically contain an adjacent aromatic residue and a proline or pipercolic acid (Pip) residue. A related family of HDAC inhibitors is the macrocyclic depsipeptide natural products, including FK228 (Romidepsin), FR901375, spiruchostatin, and largazole.^{15,16} These compounds comprise backbone ring sizes of 15–16 atoms, as compared to ring sizes of 12–13 atoms in the tetrapeptide inhibitors. Each member of the depsipeptide family contains a Zn^{2+} -coordinating thiol side chain that is initially masked either via a disulfide bond (FK228, FR901375, and spiruchostatin) or by acylation (largazole). The depsipeptides exhibit potent HDAC inhibitory activity, and FK228 in particular is the subject of ongoing human clinical trials.

To date, modification of the Zn^{2+} -coordinating functionality has been the most common strategy in studies aimed at producing potent HDAC inhibitors based on the cyclic tetrapeptide scaffold.^{6,17–20} One group studied the substitution of the epoxyketone of several known cyclic tetrapeptides with a nonalkylating hydroxamic acid functionality inspired by the

- (9) Finnin, M. S.; Donigian, J. R.; Cohen, A.; Richon, V. M.; Rifkind, R. A.; Marks, P. A.; Breslow, R.; Pavletich, N. P. *Nature* **1999**, *401*, 188–193.
- (10) Schuetz, A.; Min, J.; Allali-Hassani, A.; Schapira, M.; Shuen, M.; Loppnau, P.; Mazitschek, R.; Kwiatkowski, N. P.; Lewis, T. A.; Maglathin, R. L.; McLean, T. H.; Bochkarev, A.; Plotnikov, A. N.; Vedadi, M.; Arrowsmith, C. H. *J. Biol. Chem.* **2008**, *283*, 11355–11363.
- (11) (a) Somoza, J. R.; et al. *Structure* **2004**, *12*, 1325–1334. (b) Vannini, A.; Volpari, C.; Filocamo, G.; Casavola, E. C.; Brunetti, M.; Renzoni, D.; Chakravarty, P.; Paolini, C.; De Francesco, R.; Gallinari, P.; Steinkuehler, C.; Di Marco, S. *Proc. Natl. Acad. Sci. U.S.A.* **2004**, *101*, 15064–15069.
- (12) Shute, R. E.; Kawai, M.; Rich, D. H. *Tetrahedron* **1988**, *44*, 685–95.

- (13) (a) Horne, W. S.; Olsen, C. A.; Beierle, J. M.; Montero, A.; Ghadiri, M. R. *Angew. Chem., Int. Ed.* **2009**, in press. (b) Horne, W. S. Ph.D. Thesis, The Scripps Research Institute, 2005.
- (14) Kim, S.-D. *J. Biochem. Mol. Biol.* **1995**, *28*, 227–31.
- (15) For a recent review describing the macrocyclic depsipeptide HDAC inhibitors, see: Townsend, P. A.; Crabb, S. J.; Davidson, S. M.; Johnson, P. W. M.; Packham, G.; Ganesan, A. *Chemistry and Biology. From Small Molecules to System Biology and Drug Design*; Schreiber, S. L.; Kapoor, T. M.; Wess, G., Eds.; Wiley-VCH: Weinheim, 2007; Vol. 2, pp 693–720.
- (16) (a) Bowers, A.; West, N.; Taunton, J.; Schreiber, S. L.; Bradner, J. E.; Williams, R. M. *J. Am. Chem. Soc.* **2008**, *130*, 11219–11222. (b) Ghosh, A. K.; Kulkarni, S. *Org. Lett.* **2008**, *10*, 3907–3909. (c) Nasveschuk, C. G.; Ungermannova, D.; Liu, X.; Phillips, A. J. *Org. Lett.* **2008**, *10*, 3595–3598. (d) Numajiri, Y.; Takahashi, T.; Takagi, M.; Shin-ya, K.; Doi, T. *Synlett* **2008**, 2483–2486. (e) Ren, Q.; Dai, L.; Zhang, H.; Tan, W.; Xu, Z.; Ye, T. *Synlett* **2008**, 2379–2383. (f) Seiser, T.; Kamena, F.; Cramer, N. *Angew. Chem., Int. Ed.* **2008**, *47*, 6483–6485. (g) Taori, K.; Paul, V. J.; Luesch, H. *J. Am. Chem. Soc.* **2008**, *130*, 1806–1807. (h) Ying, Y.; Taori, K.; Kim, H.; Hong, J.; Luesch, H. *J. Am. Chem. Soc.* **2008**, *130*, 8455–8459.
- (17) (a) Gomez-Paloma, L.; Bruno, I.; Cini, E.; Khochbin, S.; Rodriguez, M.; Taddei, M.; Terracciano, S.; Sadoul, K. *ChemMedChem* **2007**, *2*, 1511–9. (b) Shivashimpi, G. M.; Amagai, S.; Kato, T.; Nishino, N.; Maeda, S.; Nishino, T. G.; Yoshida, M. *Bioorg. Med. Chem.* **2007**, *15*, 7830–7839.
- (18) Deshmukh, P. H.; Schulz-Fademrecht, C.; Procopiou, P. A.; Vigushin, D. A.; Coombes, R. C.; Barrett, A. G. M. *Adv. Synth. Catal.* **2007**, *349*, 175–183.
- (19) Murray, P. J.; Kranz, M.; Ladlow, M.; Taylor, S.; Berst, F.; Holmes, A. B.; Keavey, K. N.; Jaxa-Chamiec, A.; Seale, P. W.; Stead, P.; Upton, R. J.; Croft, S. L.; Clegg, W.; Elsegood, M. R. *J. Bioorg. Med. Chem. Lett.* **2001**, *11*, 773–776.
- (20) Furumai, R.; Komatsu, Y.; Nishino, N.; Khochbin, S.; Yoshida, M.; Horinouchi, S. *Proc. Natl. Acad. Sci. U.S.A.* **2001**, *98*, 87–92.

highly potent natural product HDAC inhibitor trichostatin A (TSA).²⁰ In all cases examined, the inhibitor potencies were significantly increased against HDAC6, while the activity against HDAC1 remained relatively unchanged. Further structure–activity relationship (SAR) studies indicated that changing the distance of the hydroxamic acid moiety from the peptide backbone by plus/minus one methylene severely decreased potency against the HDAC activity in HeLa nuclear extract.²⁰ Likewise, substitution of the ethylketone in apicidin with a hydroxamic acid increased the potency 5-fold against HeLa HDAC activity.²¹ Compounds with alternative Zn^{2+} -coordinating moieties such as methylketone, *N*-formyl hydroxylamine, mercaptoacetamide, and *o*-aminoanilide have also been studied.^{1–3,6}

Two important challenges in studying cyclic tetrapeptides as drugs are the often poor synthetic efficiency in constructing the strained 12-membered ring and the inability to control cis–trans backbone isomerization, which leads to multiple backbone conformations in solution.^{12,22,23} These difficulties have provoked several previous strategies involving modification of the cyclic tetrapeptide backbone to facilitate their synthesis and reduce their conformational heterogeneity. For instance, several groups have demonstrated that, in simple cyclic tetrapeptides, replacement of an α -amino acid with a β -amino acid to yield a 13-membered ring leads to a less strained macrocycle that successfully improves cyclization efficiencies as well as encourages the presence of a single conformation in solution.^{23,24} In the context of HDAC inhibitor cyclotetrapeptides, backbone modification strategies have included ring closure through a ring-closing metathesis reaction to yield 16-membered ring pseudo-tetrapeptides¹⁸ and replacement of backbone amide bonds with surrogate functional groups,^{13,19} unfortunately, these approaches typically resulted in compounds exhibiting poor potency in biological assays. While our studies were underway, naturally occurring HDAC inhibitor cyclic tetrapeptides containing a single β^3 -amino acid ($\alpha_3\beta$ architecture) were discovered and named the azumamides,²⁵ showing that such backbone modifications have precedent in nature.

Potent new HDAC inhibitors, especially isoform selective ones, would not only help expand our understanding of the

HDAC enzymes but also represent attractive lead compounds for drug design. Our approach toward these objectives is predicated on the hypothesis that combined structural and functional analyses of conformationally homogeneous HDAC inhibitors could shed light on the three-dimensional pharmacophoric features necessary for the future design of isoform-selective HDAC inhibitors. As a step toward these goals, here we report the design, synthesis, functional analysis, and structural characterization of a series of potent HDAC inhibitors inspired by the cyclic tetrapeptide natural products having cyclic $\alpha_3\beta$ or $\alpha_2\beta_2$ architectures (Figure 1). To survey a diverse ensemble of pharmacophoric configurations, we systematically varied the position of the β^3 -amino acid, amino acid chirality, functionalization of the Zn^{2+} -coordinating amino acid side chain, and alkylation of the backbone amide nitrogen atoms around the macrocycle. The compounds were often a single conformation in solution and exhibited potent activities against a number of HDAC isoforms as well as effective antiproliferative and cytotoxic activities against human tumor cells. High-resolution NMR solution structures were determined for a selection of the inhibitors and provide a useful means of correlating detailed structural information with potency. The structure-based approach described here is expected to provide valuable insights toward the future design of more selective HDAC inhibitors.

Results and Discussion

Design Rationale. Our design rationale centered on preparing a series of β -amino-acid-containing cyclic tetrapeptides inspired by apicidin A that, together, would cover a broad spatial range of pharmacophoric orientations. Apicidin A was chosen as our lead structure due to its combined high potency as an HDAC inhibitor and relatively weak Zn^{2+} -coordinating capability (ethylketone vs hydroxamic acid). We envisioned that the contribution from the cyclic tetrapeptide core (“cap” group) to the binding affinity would therefore be more important for apicidin A as compared to the trapoxins. Although replacement of an α -amino acid with a β -amino acid is known to encourage conformational homogeneity in simple cyclic tetrapeptides, β -amino acids have never, to our knowledge, been used in the preparation of HDAC inhibitor tetrapeptides. Therefore, to fully explore the scope of this backbone modification in the context of HDAC inhibitors we prepared a number of $\alpha_3\beta$ compounds having the β residue at three of the four possible amino acid positions as well as three compounds having two β -amino acids (the $\alpha_2\beta_2$ architecture). In the $\alpha_3\beta$ series, a variety of Zn^{2+} -coordinating moieties were examined, the side chain chirality was varied at three of the four amino acid positions, and backbone methylations were introduced at three of the four positions.

Peptide Synthesis and Preliminary Biological Evaluation. We first prepared parent peptides **1–4**, which differ in having the β -amino acid at the Trp (peptide **1**), Ala (peptide **2**), or Leu position (peptides **3** and **4**) (Figure 2). Peptides **3** and **4** differ in the presence of either an alanine (peptide **3**) or proline (peptide **4**) at position four of the peptide. In the majority of our compounds the position four residue bears the L-stereochemistry that is opposite the D-pipecolic acid residue in apicidin; in related cyclic tetrapeptide HDAC inhibitors, the stereochemistry at position four has been shown to have only a modest impact on potency.²⁶ Compounds **1–4** were prepared

- (21) Meinke, P. T.; Colletti, S. L.; Ayer, M. B.; Darkin-Rattray, S. J.; Myers, R. W.; Schmatz, D. M.; Wyvratt, M. J.; Fisher, M. H. *Tetrahedron Lett.* **2000**, *41*, 7831–7835.
- (22) (a) Chatterjee, J.; Gilon, C.; Hoffman, A.; Kessler, H. *Acc. Chem. Res.* **2008**, *41*, 1331–1342. (b) Tamamura, H.; Araki, T.; Ueda, S.; Wang, Z.; Oishi, S.; Esaka, A.; Trent, J. O.; Nakashima, H.; Yamamoto, N.; Peiper, S. C.; Otaka, A.; Fujii, N. *J. Med. Chem.* **2005**, *48*, 3280–3289. (c) Loiseau, N.; Gomis, J.-M.; Santolini, J.; Delaforge, M.; Andre, F. *Biopolymers* **2003**, *69*, 363–385. (d) Meuterms, W. D. F.; Bourne, G. T.; Golding, S. W.; Horton, D. A.; Campitelli, M. R.; Craik, D.; Scanlon, M.; Smythe, M. L. *Org. Lett.* **2003**, *5*, 2711–2714. (e) Terada, Y.; Kawai, M.; Rich, D. H. *Int. J. Pept. Protein Res.* **1989**, *33*, 3–10. (f) Kawai, M.; Pottorf, R. S.; Rich, D. H. *J. Med. Chem.* **1986**, *29*, 2409–11. (g) Kawai, M.; Jasensky, R. D.; Rich, D. H. *J. Am. Chem. Soc.* **1983**, *105*, 4456–4462.
- (23) Glenn, M. P.; Kelso, M. J.; Tyndall, J. D. A.; Fairlie, D. P. *J. Am. Chem. Soc.* **2003**, *125*, 640–641.
- (24) (a) Norgren, A. S.; Buettner, F.; Prabpai, S.; Kongsaree, P.; Arvidsson, P. I. *J. Org. Chem.* **2006**, *71*, 6814–6821. (b) Schumann, F.; Mueller, A.; Kokschi, M.; Mueller, G.; Sewald, N. *J. Am. Chem. Soc.* **2000**, *122*, 12009–12010.
- (25) (a) Maulucci, N.; Chini, M. G.; Di Micco, S.; Izzo, I.; Cafaro, E.; Russo, A.; Gallinari, P.; Paolini, C.; Nardi, M. C.; Casapullo, A.; Riccio, R.; Bifulco, G.; De Riccardis, F. *J. Am. Chem. Soc.* **2007**, *129*, 3007–3012. (b) Wen, S.; Carey, K. L.; Nakao, Y.; Fusetani, N.; Packham, G.; Ganesan, A. *Org. Lett.* **2007**, *9*, 1105–1108. (c) Nakao, Y.; Yoshida, S.; Matsunaga, S.; Shindoh, N.; Terada, Y.; Nagai, K.; Yamashita, J. K.; Ganesan, A.; van Soest, R. W. M.; Fusetani, N. *Angew. Chem., Int. Ed.* **2006**, *45*, 7553–7557.

- (26) Nishino, H.; Tomizaki, K.-Y.; Kato, T.; Nishino, N.; Yoshida, M.; Komatsu, Y. *Pept. Sci.* **1999**, *35*, 189–192.

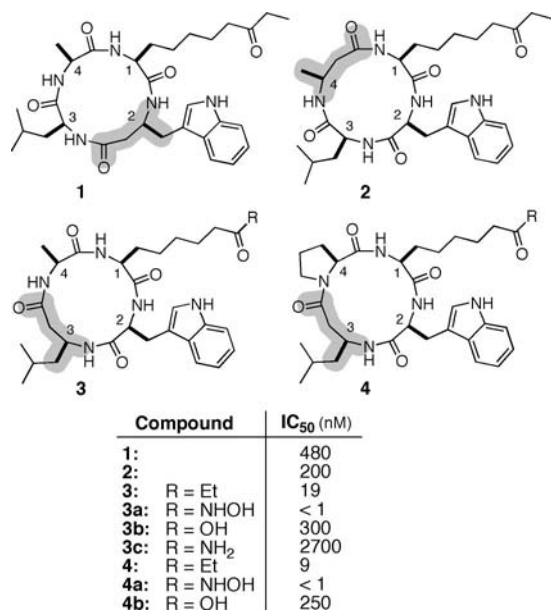


Figure 2. Chemical structures and HDAC inhibition activities (measured in HeLa cell nuclear extracts) for compounds having a cyclic $\alpha_3\beta$ -tetrapeptide architecture. The β -residue is shaded.

via standard solid-phase peptide synthesis procedures, cleavage of the linear tetramer, and cyclization under dilute conditions in solution (Scheme 1). The required protected derivative of the unnatural (*S*)-2-amino-8-oxodecanoic acid (*S*-Aoda) residue was prepared using slight modifications of a reported procedure²⁷ (Scheme S1, Supporting Information). Encouragingly, the ¹H NMR spectra (DMSO-*d*₆) for all four compounds showed a single set of sharp peaks consistent with a single peptide backbone conformation on the NMR time scale as opposed to apicidin, which adopts three conformations (~80:15:5 ratio) in DMSO-*d*₆.^{13,28} Furthermore, preliminary biological testing of the compounds for inhibition of HDAC activity in HeLa cell nuclear extract indicated that peptides **3** and **4** exhibited low nanomolar IC₅₀ values comparable to that of apicidin, whereas peptides **1** and **2** were at least an order of magnitude less potent (Figure 2). These findings confirmed that the $\alpha_3\beta$ architecture encourages conformational homogeneity and does not preclude potent HDAC inhibitory activity. As a control, the linear *N*-Boc-protected methyl ester of peptide **3** was also evaluated for HDAC inhibition activity in HeLa cell extract; this compound did not show any inhibitory activity (IC₅₀ > 10 μ M), confirming that backbone cyclization is a requirement for activity in these compounds.

We next used peptides **3** and **4** as starting points to investigate the functional effects of modifying the Zn²⁺-coordinating amino acid side chain. Peptides **3a–c**, **4a**, and **4b** were therefore prepared in a straightforward fashion by loading 2-(*N*-Fmoc-amino)-suberic acid 1-allyl ester (*N*-Fmoc-Asu-OAllyl)²⁹ via its side chain carboxylic acid onto three different types of resin (Scheme 1). Following standard solid-phase peptide synthesis procedures, allyl group deprotection, and on-resin cyclization, the peptides were cleaved from the resins and purified by RP-

HPLC to give the desired products differing only in the substitution at the Zn²⁺-coordinating residue. Introduction of the terminal hydroxamic acid moiety (peptides **3a** and **4a**) increased potency by at least 10-fold relative to the parent ethylketones **3** and **4**, which parallels previous SAR findings for analogs of other naturally occurring tetrapeptide inhibitors.^{6,20,21} On the other hand, replacement of the ethylketone with a terminal acid (peptides **3b** or **4b**) or amide (peptide **3c**) resulted in significantly decreased potency (Figure 2).

A series of peptides was next prepared to determine the functional effects of amino acid side chain chirality and backbone amide alkylation on HDAC inhibition (Figure 3). Incorporation of a D-Trp residue (compounds **2a** and **3d**) resulted in a complete loss of inhibitory activity; likewise, changing the chirality of the Aoda residue rendered peptide **3f** inactive. The importance of the Trp-Aoda chirality is not surprising considering that the aromatic and Zn²⁺-coordinating residues are generally considered the most important constituents of the pharmacophore.^{3,6} Changing the chirality of Ala in **3e** also reduced potency relative to **3**, although by a much lower extent than for **2a**, **3d**, or **3f**. It is interesting that compound **3e**, which matches the stereochemistry of apicidin, is at least 20-fold less potent than peptides **3** or **4**, which have the opposite stereochemistry relative to apicidin at the position four Ala or Pro residue; it is possible that the presence of a β^3 -amino acid causes the solution conformation of **3** and **4** to more closely mimic that of apicidin despite the greater stereochemical similarity of **3e** to the natural product. Backbone alkylations were investigated by methylating the amine moieties of Leu (peptide **3g**), Ala (peptide **3h**), and Trp (peptide **3i**). Once again, modification at Trp (**3i**) resulted in a complete loss of HDAC inhibitory activity, while modification of the Ala residue (**3h**) triggered only a modest loss of potency; methylation of the Leu residue (peptide **3g**) yielded a compound of intermediate activity (Figure 3). In general, peptide backbone methylation reduces the energetic barrier to cis–trans amide bond isomerization and thus can favor the appearance of multiple peptide conformations in solution. In this particular case, sequence **3i** showed a single set of peaks in the ¹H NMR (DMSO-*d*₆), whereas peptides **3g** and **3h** adopted multiple conformations. Taken together, these findings indicated that HDAC binding imposes strict backbone structural requirements for the Trp and Aoda residues, whereas the Ala position is relatively accommodating of backbone modifications.

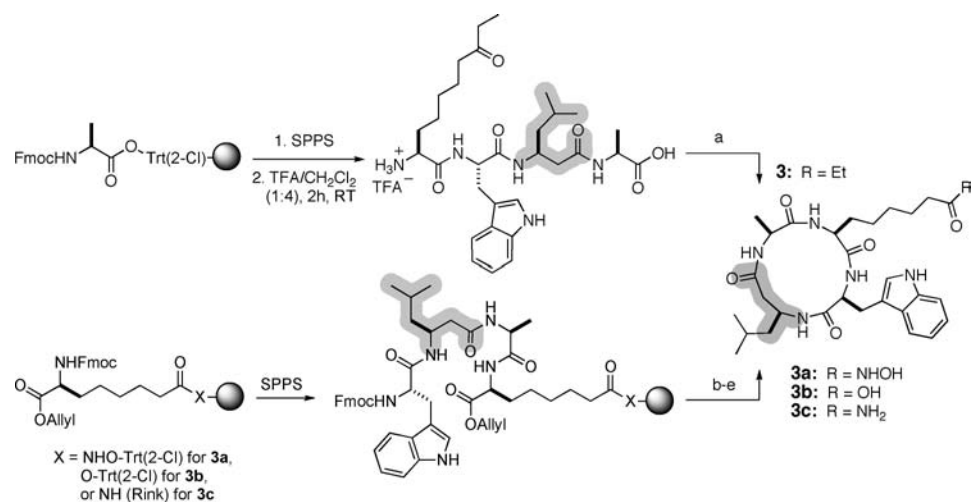
Having established that a single β -amino acid improved cyclization efficiencies and yielded generally conformationally homogeneous products, we also investigated the effects of introducing two β -residues into the cyclotetrapeptide structure ($\alpha_2\beta_2$ constructs). Compounds **5–7**, which incorporated β residues at the Ala and Leu positions (peptide **5**) or the Trp and Leu positions (peptides **6** and **7**), were therefore synthesized and characterized (Figure 4). Whereas structures **5** and **6** both adopted a single conformation in solution, peptide **7** existed as a ~3:1 ratio of two conformations, likely due to cis–trans isomerization at the Pro amide bond. In a HeLa cell nuclear extract assay peptides **6** and **7** had almost no HDAC inhibitory activity, while peptide **5** exhibited high nanomolar activity similar to that of compound **2** (β residue at Ala). These findings again suggest that the Ala region of the tetrapeptide architecture has less stringent structural requirements for HDAC inhibition activity than the Trp-Aoda region.

Bioactivity against Cancer Cell Lines. A selection of the cyclic tetrapeptide inhibitors was tested for cytotoxic activity against six cancer cell lines, including solid and liquid tumor

(27) Kim, S.; Kim, E.-Y.; Ko, H.; Jung, Y. H. *Synthesis* **2003**, 2194–2198.

(28) Kranz, M.; Murray, P. J.; Taylor, S.; Upton, R. J.; Clegg, W.; Elsegood, M. R. J. *J. Pept. Sci.* **2006**, *12*, 383–8.

(29) Kahnberg, P.; Lucke, A. J.; Glenn, M. P.; Boyle, G. M.; Tyndall, J. D. A.; Parsons, P. G.; Fairlie, D. P. *J. Med. Chem.* **2006**, *49*, 7611–7622.

Scheme 1^a

^a Conditions: (a) HATU (2 equiv), *i*Pr₂EtN (5 equiv), DMF, 0.5 mM linear peptide, 16 h, RT; quantitative conversion, 95% isolated yield. (b) 20 mol % Pd(Ph₃P)₄, CHCl₃/*N*-methylmorpholine (9:1), Ar, 4 h. (c) DMF/piperidine (3:1), 2 × 15 min. (d) HATU, *i*Pr₂EtN, 0.8% LiCl, DMF, (e) For **3a**, and **3b**: TFA/CH₂Cl₂ (1:1), 2 h, RT. For **3c**: TFA/CH₂Cl₂ (95:5), 50 min, RT. Overall isolated yields: **3** = 14%, **3a** = 15%, **3b** = 20%, **3c** = 5%.

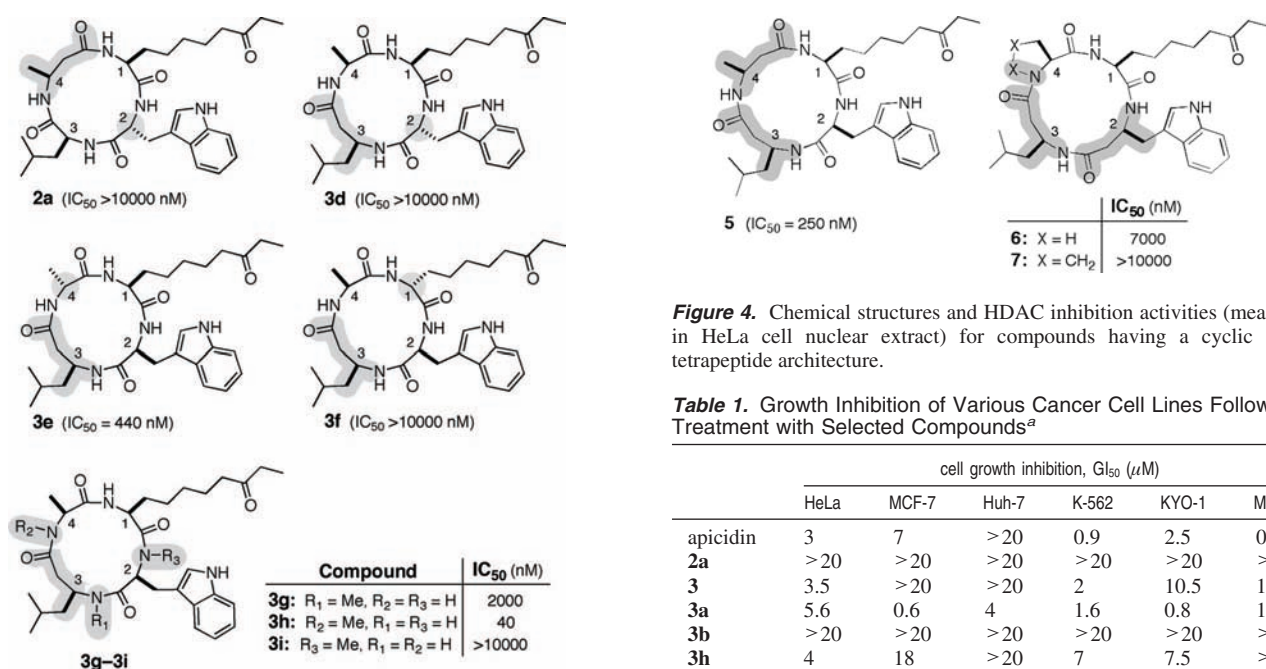


Figure 4. Chemical structures and HDAC inhibition activities (measured in HeLa cell nuclear extract) for compounds having a cyclic $\alpha_2\beta_2$ -tetrapeptide architecture.

Table 1. Growth Inhibition of Various Cancer Cell Lines Following Treatment with Selected Compounds^a

	cell growth inhibition, GI ₅₀ (μ M)					
	HeLa	MCF-7	Huh-7	K-562	KYO-1	Molt-3
apicidin	3	7	>20	0.9	2.5	0.4
2a	>20	>20	>20	>20	>20	>20
3	3.5	>20	>20	2	10.5	1.7
3a	5.6	0.6	4	1.6	0.8	1.6
3b	>20	>20	>20	>20	>20	>20
3h	4	18	>20	7	7.5	>20
4	2.1	20	>20	1.5	10	0.35
5	>20	>20	>20	>20	>20	>20

^a HeLa (cervical cancer), MCF-7 (breast cancer), Huh-7 (human hepatocarcinoma), K-562 (chronic myeloid leukemia), KYO-1, Molt-3 (chronic myeloid leukemia).

Figure 3. Chemical structures and HDAC inhibition activities (measured in HeLa cell nuclear extracts) for $\alpha_3\beta$ compounds having varied amino acid chirality or a backbone amide methylation. The β residue, chiral center being altered, and amine being methylated are shaded.

cells (Table 1). The ethylketone-containing compounds that were most active against HeLa cell nuclear extract (apicidin, **3**, and **4**) exhibited significant cell-specific cytotoxicity. The hydroxamic-acid-containing peptide **3a** inhibited the growth of all the cell lines tested, consistent with its high potency against HDAC activity in HeLa nuclear extract. It is noteworthy that although peptide **3a** was at least 10-fold more active than the other compounds against HeLa cell nuclear extract, compounds **3**, **3a**, **3h**, and **4** were approximately equipotent in cytotoxic activity against HeLa cells (Table 1), demonstrating that differences in HDAC inhibition activity in HeLa nuclear extract does not necessarily correspond to similar differences in cytotoxic activity. The high nanomolar (**3b** and **5**) as well as inactive (**2a**) inhibitors of HDAC activity in HeLa nuclear extract did not

inhibit cell growth in any of the cell lines tested. It is interesting to note that, in general, the compounds exhibit higher potency in leukemia cell lines, such as K-562, KYO-1, and Molt-3 cells. It is nonetheless encouraging that some of the inhibitors are capable of crossing cellular and nuclear membranes and exhibiting potent cytotoxic activity against tumor cell lines.

Bioactivity against Isolated HDAC Isoforms. We further assayed a selection of the inhibitors against a panel of recombinant human HDAC isoforms (HDACs 1–10) to gain knowledge about the specific interactions of the various cyclotetrapeptides with these enzymes (Table 2). The $\alpha_3\beta$ ethylketone-containing compounds (**3**, **3h**, and **4**) exhibited comparable potencies to apicidin against HDACs 1, 2, 4, 5, 6, 7, 9,

Table 2. Activities of Selected Compounds against Recombinant Human HDAC Isoforms 1–10

compound	HDAC inhibition, IC ₅₀ (nM) ^a										
	HeLa	class I				class IIa				class IIb	
		HDAC1	HDAC2	HDAC3	HDAC8	HDAC4	HDAC5	HDAC7	HDAC9	HDAC6	HDAC10
apicidin	9	18	35	100	750	> 10 000	80	> 10 000	15	> 10 000	30
3	19	35	30	150	2,200	> 10 000	70	> 10 000	30	> 10 000	20
3a	<1	1.5	5	25	120	> 10 000	2.5	> 10 000	0.6	30	0.2
3b	300	100	200	600	2300	> 10 000	700	> 10 000	550	2300	280
3h	40	50	40	550	2000	> 10 000	60	> 10 000	25	> 10 000	28
4	9	12	40	280	1500	> 10 000	50	> 10 000	22	> 10 000	15
4a	<1	0.6	3.5	35	180	> 10 000	n.d. ^b	> 10 000	n.d.	35	n.d.
5	250	300	400	1,500	> 10 000	> 10 000	2,800	> 10 000	400	> 10 000	400

^a Assays were performed at least in duplicate. ^b Not determined.

and 10 and decreased activities relative to apicidin against HDACs 3 and 8. The 14-membered ring $\alpha_2\beta_2$ compound **5**, on the other hand, exhibited potencies values lowered by at least 10-fold across the entire panel of enzymes when compared to apicidin. Similarly, the carboxylic-acid-containing compound **3b** also generally exhibited higher IC₅₀ values against the panel of HDACs than apicidin, consistent with its poorer potency in HeLa nuclear extract. The hydroxamic acids (**3a** and **4a**) exhibited consistently low nanomolar potencies across the panel of enzymes. HDAC6 was sensitive only to the hydroxamic-acid-containing peptides (**3a** and **4a**), which is in accordance with the findings of Yoshida and co-workers, who reported a similar observation when substituting the epoxyketone in trapoxin with a hydroxamic acid.²⁰ These results indicate that potent inhibition of HDAC6 requires a strong Zn²⁺-coordinating moiety, which in turn suggests that the cyclic peptide “cap” provides a less significant contribution to the binding of ligands to this particular HDAC isoform. There was no apparent trend in the potency of our compounds against HDACs within each of the classes: I, IIa, and IIb (Table 2). Specifically, our inhibitors were effective against class-IIb HDAC10 but less effective against class-IIb HDAC6. The same was true for class-I HDACs 1, 2, and 3 vs HDAC8 and class-IIa HDACs 5 and 9 vs HDACs 4 and 7. It is not yet clear if class-IIa HDACs are in fact functional deacetylases in vivo as studies have shown that their intrinsic HDAC activity is considerably lower than HDACs 1 and 3, and their ability to deacetylate histone substrates has been linked with their association with HDAC3 in multiprotein complexes.^{5,30} Our results nonetheless clearly demonstrate that strong inhibitors against a single HDAC within one of the classes I or IIb is not necessarily a strong inhibitor of the other isoforms in that class. Likewise, a lack of activity against a particular enzyme isoform does not necessarily rule out potent inhibitory activities against other isoforms of the same class, indicating that a thorough investigation of inhibitor activities is crucial when searching for subtype-selective HDAC inhibitors. Although it is possible that the generally high IC₅₀ values observed against HDAC6 and HDAC8 compared to the other isoforms result from slower inhibitor binding kinetics for these isoforms, this explanation seems unlikely considering the relatively potent inhibition by the hydroxamic-acid-containing peptides **3a** and **4a**. It is perhaps not surprising that inhibition profiles are inconsistent within the HDAC classes, considering

that HDAC classification is based on sequence similarity to the yeast factors yRPD3 and yHDA1 rather than enzymatic function.

Our data reveal interesting correlations between the whole cell cytotoxicity profiles and the HDAC isoform activities. For example, apicidin was a stronger inhibitor of MCF-7 and KYO-1 growth than the structurally similar 13-membered ring compounds **3**, **3h**, and **4**. Since apicidin is 2–5 times more potent toward HDACs 3 and 8 as compared to compounds **3**, **3h**, and **4**, while similar activities were observed toward all other HDAC isoforms, this may suggest that inhibition of HDACs 3 and/or 8 is essential for growth inhibition in MCF-7 and KYO-1 cells. However, interactions of apicidin with entirely different targets cannot be excluded as an explanation for this observation. Furthermore, the correlation between the IC₅₀ values obtained for our compounds against HeLa nuclear extract and the recombinant HDAC isoforms strongly suggest that the enzymatic activity in the HeLa nuclear extract originates predominantly from HDACs 1, 2, and 3. Precedents for a high abundance and a dominant activity of HDAC1 have been reported for other cell types,^{31,32} knocking down HDAC1 in embryonic stem cells from mice, for instance, resulted in hyperacetylation of histones H3 and H4, suggesting that the other HDAC isoforms could not compensate for the missing HDAC1.³² It is therefore likely that an initial screening of compounds against HeLa cell extracts may considerably bias the search for potent inhibitors, particularly against inhibitors of class-II HDACs.

Structural Determinations by Multidimensional NMR. The functional HDAC inhibition data described above is informative but can be rendered much more powerful if combined with high-resolution structural determination of the inhibitors because such an analysis affords the possibility to carefully scrutinize how different bioactivities correlate with the precise pharmacophoric arrangements of different inhibitors. Structures were therefore determined for a number of the inhibitors to garner a detailed understanding of the three-dimensional orientations of their pharmacophoric elements. We restricted our structural analyses to those compounds that were a single conformation in solution and expected to provide useful structural information (for a series of compounds that differed only in Zn²⁺-coordinating moieties, only the parent compound was subjected to structural determination). Fortunately, compounds **1–6** were all a single conformation in DMSO-*d*₆ at 295 K, providing a broad range of activities and pharmacophoric configurations for investigation. Amide backbone and side chain proton assignments were

(30) (a) Lahm, A.; Paolini, C.; Pallaoro, M.; Nardi, M. C.; Jones, P.; Neddermann, P.; Sambucini, S.; Bottomley, M. J.; Lo Surdo, P.; Carfi, A.; Koch, U.; De Francesco, R.; Steinkuehler, C.; Gallinari, P. *Proc. Natl. Acad. Sci. U.S.A.* **2007**, *104*, 17335–17340. (b) Fischle, W.; Dequiedt, F.; Hendzel, M. J.; Guenther, M. G.; Lazar, M. A.; Voelter, W.; Verdin, E. *Mol. Cell* **2002**, *9*, 45–57.

(31) Gopal, Y. N. V.; Arora, T. S.; Van Dyke, M. W. *Chem. Biol.* **2007**, *14*, 813–823.

(32) Lagger, G.; O’Carroll, D.; Rembold, M.; Khier, H.; Tischler, J.; Weitzer, G.; Schuettengruber, B.; Hauser, C.; Brunmeir, R.; Jenwein, T.; Seiser, C. *EMBO J.* **2002**, *21*, 2672–2681.

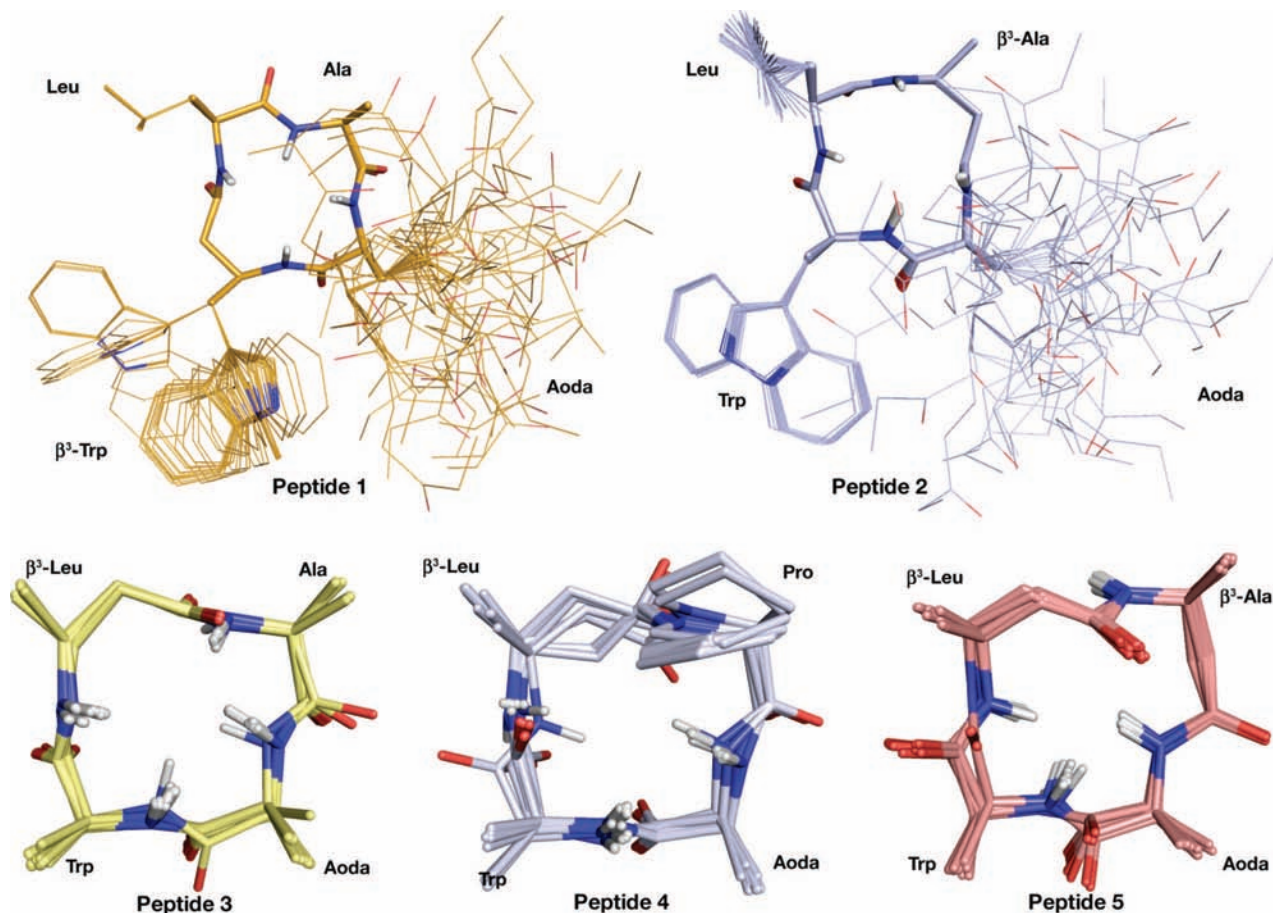


Figure 5. NMR solution structures (DMSO- d_6) for selected potent peptides. For peptides **1** and **2** all side chain atoms are shown, whereas side chain atoms beyond the C_β have been omitted for clarity in compounds **3–5**.

accomplished via two-dimensional TOCSY NMR. Two-dimensional ^1H ROESY NMR allowed identification of NOEs, which were then translated to three categories of distances: strong, ≤ 2.7 Å; medium, ≤ 3.5 Å; and weak, ≤ 4.5 Å. Special care was taken to search for the presence of cis amide bonds, including allowing the amide bonds to freely rotate in structure calculations and scanning the ROESY spectra at high intensity for NOEs indicative of cis amides such as neighboring residue H_α – H_α coupling, H_α – H_β coupling, H_α – H_{β_3} coupling, or H_β – H_{β_3} coupling (“ β_3 ” refers to the extra methylene carbon in the β^3 -amino acids).

Of the $\alpha_3\beta$ compounds for which we determined structures, peptides **1** (β -Trp residue) and **2** (β -Ala residue) both adopted a single rigid conformational ensemble in solution, whereas peptides **3**, **3i**, and **4** (β -Leu residue) each exhibited a generally more flexible conformational ensemble and adopted two families of structures that in all cases resulted from different rotations of one of the amide linkages relative to the plane of the backbone (Figures 5 and 6). Although the amide rotation had relatively little effect on the positions of backbone atoms or C_α – C_β vectorial alignments for the Aoda-Trp-Leu pharmacophore region (Figure 5), this observation suggests that a β residue at the Leu position of the cyclic tetramers may give rise to increased conformational heterogeneity. Of the $\alpha_2\beta_2$ compounds (**5** and **6**), peptide **5** adopted a single conformation in solution (Figure 5) while peptide **6** exhibited two conformational families differing in the rotation of the Aoda-Trp amide bond relative to the plane of the backbone (Figure 6b). No evidence of cis amide bonds was found for any of the

determined structures except peptide **3i**, which contained a cis configuration at its N -methylated amide position (Figure 6a).

Pair-Fitting Analyses To Correlate Structures with Bioactivities. Having determined high-resolution structures for a number of cyclic tetrapeptides of varying HDAC inhibitory activity, we next attempted to relate the observed molecular structures with their corresponding bioactivities. As indicated by the SAR described above and by previous studies with other HDAC inhibitors,^{3,6} the most important constituents of the cyclic tetrapeptide pharmacophore comprise the Aoda, Trp, and Leu side chains as well as the Aoda-Trp amide bond. Eight backbone atoms corresponding to this pharmacophore (the C_α and C_β atoms of the Aoda, Trp, and Leu side chains as well as the Trp N_α atom and the Aoda carbonyl carbon) were therefore used for the pair-fitting analyses described below in the hopes of identifying structural similarities between compounds with comparable inhibition profiles. The analyses were carried out using a representative structure from each compound or conformational family (in the cases where two families of structures had been observed in the structure calculations, both were considered when conducting the structural analyses).

Each peptide for which we determined an NMR structure was pair fit to a representative structure of **3**; peptide **3** was chosen as the basis for fitting because it was the parent compound for our most active HDAC inhibitors. The compounds that overlaid well (rmsd < 0.3 Å) in this analysis (peptides **2**, **3**, **4**, and **5**) corresponded to those that exhibited more potent inhibition of HDAC activity in HeLa cell nuclear extract, while those compounds with higher rmsd values

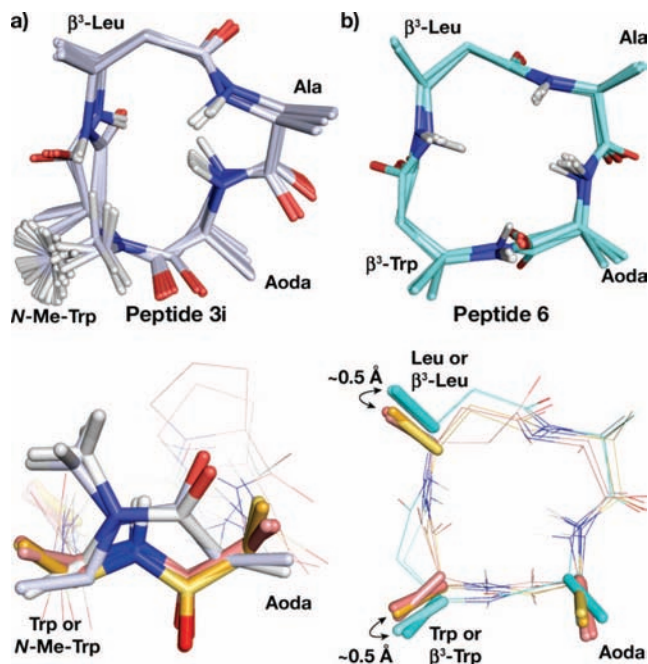


Figure 6. NMR solution structures for peptides **3i** and **6** and the likely structural reasons for their low potencies. In all structures side chain atoms beyond the C_{β} have been omitted for clarity. (a) The NMR structure for peptide **3i** is shown at the top. At bottom, an overlay illustrates that the cis amide bond in compound **3i** (white, representative structures from the two structural families) causes the Trp and Aoda C_{α} - C_{β} vectors to project in the same plane as the peptide backbone, while the C_{α} - C_{β} vectors in the potent compounds **3** (yellow, representative structures from the two structural families) and **4** (pink, representative structures from the two structural families) project upward from the backbone plane. The *N*-methyl group may also lead to steric clashes with the HDAC binding pockets. (b) The NMR structure for peptide **6** is shown (top). At bottom, an overlay demonstrates that the β -Trp moiety in peptide **6** (cyan, representative structures from the two structural families) leads to a greater distance between the side chains of the Leu and Trp residues than in the more potent compounds **3** (yellow, representative structures from the two structural families) and **4** (pink, representative structures from the two structural families).

(peptides **1**, **3i**, and **6**; rmsd > 0.3 Å) corresponded to the poorer HDAC inhibitors (Table 3). Furthermore, inspection of the overlay allowed us to identify a correlation of the side chain C_{β} - C_{β} distances with the relative HDAC inhibition activities (the same correlation was observed for distances between C_{α} atoms but was less pronounced) (Figures 6 and 7a). Specifically, the most potent inhibitors were those having distances between the Aoda and Trp C_{β} atoms (“distance A” in Table 3 and Figure 7a) of 5.0–5.3 Å and distances between the Trp and Leu C_{β} atoms (“distance B” in Table 3 and Figure 7a) of 5.1–5.3 Å. Peptides having C_{β} - C_{β} distances significantly outside of these optimal ranges exhibited poor potency in the bioassays, as exemplified by compounds **1** and **6** having distance B measurements of >6 Å (Figure 6b). Although the C_{β} - C_{β} distances in compound **3i** are not drastically outside the optimal region, the rmsd for this compound against peptide **3** is very high due to the poor overlay of the cis Aoda-Trp amide in **3i** compared to the trans amide in **3**; the cis amide also enforces that the Trp and Aoda C_{α} - C_{β} vectors in **3i** are in the same plane as the peptide backbone, as opposed to C_{α} - C_{β} vectors projecting upward from the plane in the compounds having a trans amide (Figure 6a). The *N*-methyl group in **3i** may also lead to steric clashes with the HDAC binding pockets.

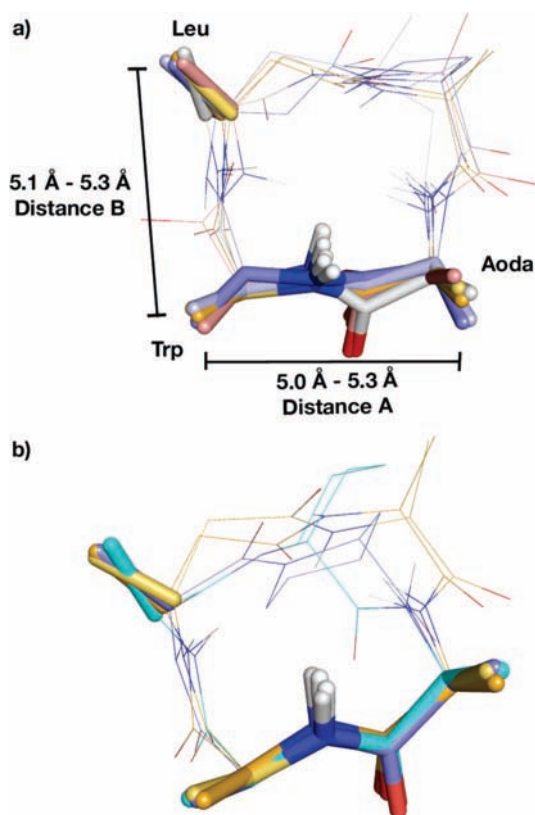


Figure 7. Structural overlays. (a) Superposition of active compounds **2**, **3** (representative structures from the two structural families), **4** (representative structures from the two structural families), and **5**. Atoms present in the pharmacophore are shown in sticks for emphasis. Side chains have been omitted for clarity but are labeled. The distances shown are those determined to be ideal for potent HDAC inhibition. (b) Overlay of the DMSO- d_6 apicidin structure (purple), crystallographic apicidin structure (cyan), and representative structures of the two structural families of peptide **3** (yellow and gold). Although compound **3** comprises an $\alpha_3\beta$ architecture and apicidin an α_4 architecture, the pharmacophoric regions of the molecules (shown with sticks) overlay very well.

The natural product apicidin also exhibited a low rmsd and C_{β} - C_{β} distances in the optimal ranges depending on which of its three reported molecular structures were used for the analysis (Figure 7b). Two somewhat different NMR structures have been determined for apicidin in pyridine- d_5 ³³ and DMSO- d_6 ,²⁸ both having all the backbone amides in the trans configuration; a crystallographic apicidin structure having a single cis amide bond has also been reported.²⁸ The DMSO- d_6 NMR structure and the crystal structure both adopt conformations that should furnish potent HDAC inhibitors based on our analysis; recent studies in our laboratory have suggested that the conformation containing the cis amide is more likely the biologically relevant structure.¹³ That the pharmacophoric region of the α_4 natural product apicidin overlaid well on that of the $\alpha_3\beta$ peptide **3** (Figure 7b) is a testament to the present strategy for preparing new HDAC inhibitors. On the other hand, the rmsd value for the natural product azumamide E against peptide **3** is quite high but can be ascribed to the retro-reverso configuration of the azumamides having the reversed absolute stereochemistry and inverse direction of amide bonds around the ring relative to **3**. The pharmacophoric region C_{β} - C_{β} distances in azumamide E

(33) Singh, S. B.; Zink, D. L.; Polishook, J. D.; Dombrowski, A. W.; Darkin-Rattray, S. J.; Schmatz, D. M.; Goetz, M. A. *Tetrahedron Lett.* **1996**, *37*, 8077–8080.

Table 3. Compilation of RMSD Values and C_{β} – C_{β} Distances Used for Structural Analysis

compound	rmsd ^a	distance A ^b (Å)	distance B ^c (Å)
1	0.377	5.10	6.08
2	0.219	5.15	5.12
3 (family 1)	NA	4.98	5.28
3 (family 2)	0.175	5.03	5.09
3i (family 1)	0.937	5.59	5.49
3i (family 2)	1.026	5.38	5.22
4 (family 1)	0.255	5.23	5.20
4 (family 2)	0.295	5.02	5.24
5	0.255	4.80	5.31
6 (family 1)	0.401	4.93	6.31
6 (family 2)	0.673	5.14	6.37
apicidin, crystal	0.212	5.33	5.03
apicidin, NMR (DMSO- <i>d</i> ₆)	0.143	5.14	5.19
apicidin, NMR (pyridine- <i>d</i> ₅)	0.562	5.55	5.34
azumamide	0.589	4.76	5.26

^a rmsd values were calculated with the MacPymol pair-fitting command using a representative structure of peptide **3a**. The pair-fitting analysis included eight atoms: the C_α and C_β of Aoda, Trp and Leu residues, as well as the Trp N_α and Aoda carbonyl C. $\text{rmsd} = \{[\sum(d_{ii})^2]/N\}$, where d_{ii} = the distance between the *i*th atom in structure 1 and the *i*th atom in structure 2. ^b Calculated as the distance between Aoda C_β and Trp C_β. ^c Calculated as the distance between Trp C_β and Leu C_β.

nonetheless remain close to the optimal values established by our analysis (Table 3). It is interesting that the $\alpha_3\beta$ peptides described here more closely match the structure of the α_4 natural product apicidin than the $\alpha_3\beta$ natural product azumamide E, although this likely is again due to the retro-reverso configuration of the azumamides. Finally, the pair-fitting analysis described here may be useful for the future structure-based design of potent HDAC inhibitors.

Conclusion

The functional and structural characterization of potent $\alpha_3\beta$ cyclic tetrapeptide HDAC inhibitors described here is expected to provide useful insights toward the future design of more selective HDAC inhibitors. Although the relative positions of the Trp and Aoda residues (and their counterparts in other natural product HDAC inhibitors) are typically the focus of SAR studies, the position of at least a third side chain is also important for potency based on our analysis, so selectivity between the HDAC isoforms might therefore be attained by varying these three positions of the cyclic tetrapeptide scaffold. Our investigation suggests that hydroxamic acids, which have been explored extensively as HDAC inhibitors, are excellent for obtaining potent compounds but are unlikely to be useful in the search for subtype specific HDAC inhibitors due to their indiscriminate binding across the HDAC family, especially when attempting to differentiate between highly homologous isoforms, such as HDAC1 vs HDAC3.³⁴ Ethylketones and carboxylic acids should

be considered more promising for this purpose, especially when combined with a cyclic tetrapeptide “cap” group that adds to the overall binding affinity of the inhibitor. The data presented here also demonstrate that one cannot be sure to have a selective inhibitor across the whole panel of HDAC enzymes without testing for activity against each isoform, which complicates the search for novel inhibitors considerably. Screening of compound libraries against the whole panel of recombinant enzymes is not currently an economically feasible solution, but the carboxylic-acid-derivatized tetrapeptide compounds have considerable future potential as discovery tools owing to their amenability to the preparation of one-bead-one-compound combinatorial libraries via the solid-phase synthesis protocols described herein.

Acknowledgment. Coordinates for the NMR structures reported in this manuscript have been deposited at the BMRB databank (www.bmrb.wisc.edu, accession codes 20064–20070). We thank Prof. Joel Gottesfeld and Dr. David Herman for helpful discussions and technical assistance, Drs. Dee Huang and Laura Pasternack for assistance with multidimensional NMR experiments, Dr. W. Seth Horne for assistance writing the Aoda residue for CNS, Dr. Sheo Singh for providing coordinates of the published NMR structure of apicidin in pyridine-*d*₅, Dr. Michael Kranz for providing coordinates of the calculated lowest energy conformations of apicidin, Dr. Giuseppe Bifulco for providing coordinates of the NMR structure of azumamide E, the TSRI Mass Spectrometry Facility for high-resolution mass spectral analyses, and Dr. L. J. Leman for assistance in manuscript preparation. We acknowledge the NASA Earth and Space Science Fellowship Program (Grant NNX07AR35H) (J.M.B.) for a predoctoral fellowship. A.M. thanks the Spanish Ministry for Science and Education for a Fulbright/MEC postdoctoral fellowship. CAO thanks the Lundbeck Foundation and the Danish Research Council for Technology and Production Sciences (274-06-0317) for postdoctoral fellowships and the Danish Independent Research Council for a Young Researchers Award. This work was supported in part by a grant from the National Institute of General Medical Sciences (GM52190) and the Skaggs Institute for Chemical Biology.

Note Added in Proof. The crystallographic structure of the human HDAC4 catalytic domain has recently been reported. See: Bottomley, M. J.; Lo Surdo, P.; Di Giovine, P.; Cirillo, A.; Scarpelli, R.; Ferrigno, F.; Jones, P.; Neddermann, P.; De Francesco, R.; Steinkuehler, C.; Gallinari, P.; Carfi, A. *J. Biol. Chem.* **2008**, *283*, 26694–26704.

Supporting Information Available: Schemes S1 and S2, experimental procedures for the amino acid syntheses, compound characterization data, ROESY tables, and ¹H NMR spectra for selected compounds. This material is available free of charge via the Internet at <http://pubs.acs.org>.

(34) Chou, C. J.; Herman, D.; Gottesfeld, J. M. *J. Biol. Chem.* **2008**, *283*, 35402–35409.